FORMULATION OF PREDICTION MODEL FOR WORKING FLUID TEMPERATURE IN A VERTICAL PARABOLOID-SHAPED THERMAL ENERGY STORAGE TANK DURING STAND-ALONE OPERATION

Khurana H.[a,*], Majumdar R.[b] and Saha S.K.[a]
[a]Department of Mechanical Engineering, Indian Institute of Technology Bombay, Mumbai- 400076, INDIA.
E-mail : 174100020@iitb.ac.in
[b]EECP, National Institute of Advanced Studies, Bengaluru-560012, INDIA.

ABSTRACT

Stand-alone operation of thermal energy storage (TES) is crucial for domestic hot water applications, in which the performance of the storage system is significantly affected by the natural convection phenomenon. In the present study, a two-dimensional axisymmetric numerical model is developed for the detailed simulation of stand-alone TES. Findings of a previous study indicates that sloped wall TES exhibits better heat retention capabilities owing to lower thermal losses as compared to the cylindrical TES. The present study considers a paraboloid shaped TES with an aspect ratio (*AR*) of 1.66 as a reference configuration for further investigation. The numerical simulations show the evolution of thermal stratification in the paraboloid TES, during the stand-alone period spanning over 6 h. An average temperature gradient of 2.06 °C/m is observed along the height of the vertical storage tank over the aforesaid 6 h period. Based on the detailed simulations, an effective prediction model for the considered TES configuration is formulated using a four-parameter three-level Box-Behnken Design (BBD), which is one of the Response Surface Methodologies (RSM) to evaluate the water temperature distribution inside the storage tank. The formulated prediction equation covers an adequately wide range of values for the chosen four parameters, namely the charging temperature, ambient temperature, height ratio and storage time ratio, considering realistic domestic and industrial requirements. Analysis of variance (ANOVA) is performed to select the statistically significant terms and a reduced prediction equation is generated. From the comparison of the results obtained through the detailed simulations and the prediction equation, it is concluded that the formulated reduced prediction equation can predict the thermal characteristics and evolution of water temperature profiles within the stand-alone paraboloid-shaped TES with adequate accuracy.

NOMENCLATURE

C_p	[J/kg.K]	Specific heat
g	[m/s^2]	Acceleration due to gravity
H	[m]	Height of TES
h	[W/m^2.K]	Heat transfer coefficient
Nu	[-]	Nusselt number
P	[N/m^2]	Pressure
Pr	[-]	Prandtl number
q	[W]	Heat transfer rate
R^2	[-]	Coefficient of determination
r	[-]	Radial direction
Ra	[-]	Rayleigh number
t	(s)	Time
T	[°C]	Temperature
u	[m/s]	Velocity
u_r	[m/s]	Radial velocity
u_z	[m/s]	Axial velocity
z	[-]	Axial direction
Special characters		
λ	[W/m. K]	Thermal conductivity
β	[1/K]	Thermal expansion coefficient
μ	[kg/m. s]	Dynamic viscosity
ρ	[kg/m^3]	Density
Subscripts		
insl		Insulation
amb		Ambient
fi		Water initial
f		Water
ini		Initial
w		Wall
max		Maximum
min		Minimum

INTRODUCTION

Thermal energy storage (TES) systems mitigate the temporal mismatch between the supply and demand of solar energy [1, 2]. TES is crucial for several industrial, commercial, and domestic applications that utilize sensible heat [3]. Due to the ample availability, less expenses and high volumetric heat capacity, water is used as the working fluid in most cases [4]. When there is no flow into/from the storage tank, it is considered as the stand-alone condition of the storage tank. Velocity and temperature boundary layers are developed during the stand-alone operation along the lateral walls of the storage tank, owing to the convective heat transfer between the water inside the tank and the surroundings. Gradually, it leads to the formation of thermal stratification in the storage tank [5]. Published literature primarily focuses on the vertical cylindrical storage tanks with the temperature and heat flux conditions imposed on to the walls [6-8]. However, recent studies have shown that paraboloidal tank geometry offers superior performance in terms of thermal stratification as compared to the circular truncated-cone and cylindrical geometries, ensuring better thermodynamic quality of the stored working fluid in the upper section of the TES [9].

To address the temporal mismatch between the thermal energy availability and demand, caused by the intermittent nature of insolation, it is essential to understand the thermal characteristics, *i.e., evolution of thermal stratification,*

entropy generated during the operation, energy storage efficiencies and *heat retention capabilities of TES*. Consequently, a precise evaluation of water temperature distribution within the TES is crucial. The objective of this study is to formulate a prediction model to estimate the water temperature distribution for an improved geometrical configuration of TES tank (paraboloidal shape) operating in stand-alone mode. Recently, a seven-parameter three-level Box Behnken Design-based prediction model was developed to facilitate accurate prediction of working fluid temperature in a vertical cylindrical sensible heat storage tank [10]. The results of the reduced prediction model were validated against the detailed simulations as well as the experimental data obtained from an in-house facility housed at IIT Bombay. The reduced BBD-based models are devoid of computational overhead and save the resources that would have been spent otherwise in the repeated experimental trials. Based on the trends of water temperature distribution inside vertical cylindrical TES captured in the experimental study [10], the quadratic model approach of BBD is found suitable to find the factors of the model in this study, as against the linear model or the OFAT (one factor at a time) approach. Following the procedural steps delineated in detail in the previous study [10], a four-parameter three-level BBD-based prediction equation is formulated in this work. In the previous study, the seven parameters considered for the BBD simulation were volume of tank, aspect ratio, charging temperature, ambient temperature, thickness of insulation, height ratio and storage time ratio. Detailed statistical analysis (including ANOVA) highlighted four out of the seven parameters that are quintessential in terms of model considerations. These are charging temperature, ambient temperature, height ratio and storage time ratio.

In this study, the prediction model for a paraboloid-shaped TES tank considers these dominant four parameters only, to further reduce the computational efforts. Considering the broad range of operating conditions based on domestic and industrial applications, a scaling-based prediction equation is formulated for the paraboloidal storage tank. **Figure 1** depicts the conceptual systemic diagram comprising the paraboloid TES tank and other key components.

Geometrical Parameters of the TES Tank

Paraboloidal shaped storage tank configuration with an aspect ratio of 1.66 has been chosen based on a previous study [9]. Based on the reported literature, the ranges of chosen process parameters are defined by looking at average daily domestic and industrial hot water requirements. For domestic purposes, storage tanks of 160-1000 L capacity are offered by industrial manufacturers [11]. A paraboloidal storage tank of 600 L capacity is considered for further simulations. An insulation thickness of 40 mm is considered in this study, considering the lower end of the range generally provided by the TES manufacturers (40-100 mm) [12].

Choice of Other Operating Parameters

Selection of range for the key process parameters is an important consideration to develop an adequately accurate response prediction model [13]. Based on the domestic hot water (DHW) requirements, the range of charging temperature is selected as 50-90 °C. The range of average ambient temperature (23-36 °C) is selected considering the weather of Mumbai, India. The maximum storage time of 6 h has been selected as per the hot water demands during the evening period (18:00 - 23:00 h) [14]. All the numerical runs suggested by the BBD matrix are carried out for the 6h duration. The value of *Ra* for all the numerical runs varies between 2.9×10^{10} and 1.1×10^{12}. **Table 1** presents the selected process parameters and their values at three levels.

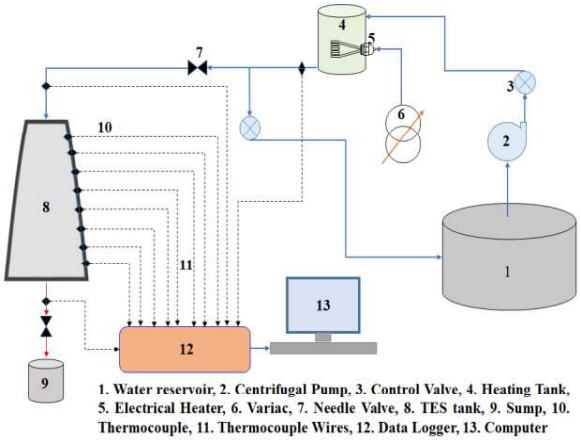

Figure 1 Conceptual systemic diagram comprising paraboloidal TES tank

Table 1: Levels and respective values of process parameters

Process parameter	Units	-1 Level	0 Level	+1 level
Charging temperature (A)	°C	50	70	90
Ambient temperature (B)	°C	23	29.5	36
Height ratio (C)	-	0	0.5	1
Storage time ratio (D)	-	0.027	0.5135	1

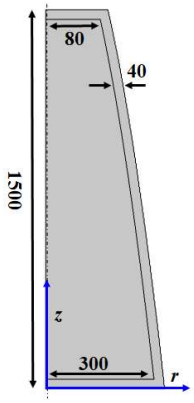

Figure 2 Axisymmetric two-dimensional numerical domain of paraboloidal TES (all dimensions are in mm) (not to scale)

NUMERICAL APPROACH

Geometrical Domain

A numerical model is developed for the stand-alone paraboloidal storage tank, to analyze the evolution of the

volumetric temperature distribution of water inside TES. A two-dimensional axisymmetric numerical domain is considered as depicted in **Figure 2**. The storage tank under stand-alone operation continuously loses thermal energy to the ambient due to natural convection, which necessitates the selection of an appropriate model to assess the flow state of the working fluid (water) inside TES. The reported study considers the flow to be laminar up to a critical *Ra* value of 10^{13} [15]. The *Ra* evaluated for every case presented in this study is considerably lesser than the critical value of *Ra* reported in the literature. Therefore, laminar flow regime has been considered for the fluid flow simulations in the present study.

Numerical Formulation

The mass, momentum and energy equations govern the heat transfer and fluid flow phenomenon inside the TES tank. The Boussinesq approximation is applied to the axial momentum conservation equation, to incorporate the buoyancy effects. Water has been treated as an incompressible and Newtonian fluid. Uniform initial water temperature is considered inside the storage tank. Water has been assumed to have isotropic and constant thermophysical properties over the range of temperature considered. The effect of tank wall is neglected as the tank wall is much thinner as compared to the average diameter of storage tank. The governing equations used are specified below [10].

***Conservation of mass*:**

$$\frac{1}{r}\frac{\partial(ru_r)}{\partial r}+\frac{\partial u_z}{\partial z}=0 \tag{1}$$

***Conservation of axial and radial momentum equations*:**

$$\rho_f\left(\frac{\partial u_r}{\partial t}+u_r\frac{\partial u_r}{\partial r}+u_z\frac{\partial u_z}{\partial z}\right) = -\frac{\partial P}{\partial r} + \mu_f\left(\frac{1}{r}\frac{\partial}{\partial r}\left(r\frac{\partial u_r}{\partial r}\right)-\frac{u_r}{r^2}+\frac{\partial^2 u_r}{\partial z^2}\right) \tag{2}$$

$$\rho_f\left(\frac{\partial u_z}{\partial t}+u_r\frac{\partial u_z}{\partial r}+u_z\frac{\partial u_z}{\partial z}\right) = -\frac{\partial P}{\partial z}+\mu_f\left(\frac{1}{r}\frac{\partial}{\partial r}\left(r\frac{\partial u_z}{\partial r}\right)+\frac{\partial^2 u_z}{\partial z^2}\right) + \rho_f g\beta_f\left(T_f-T_{fi}\right) \tag{3}$$

***Conservation of energy*:**

$$\rho_f c_p\left(\frac{\partial T_f}{\partial t}+u_r\frac{\partial T_f}{\partial r}+u_z\frac{\partial T_f}{\partial z}\right) = \frac{1}{r}\frac{\partial}{\partial r}\left(\lambda_f r\frac{\partial T}{\partial r}\right)+\frac{\partial}{\partial z}\left(\lambda_f\frac{\partial T}{\partial z}\right) \tag{4}$$

The boundary conditions of the stand-alone TES considered are,

(i) No-slip condition at the wall of TES, $\boldsymbol{u|_w = 0}$ (5)

(ii) Coupled thermal boundary condition, (6)

$\boldsymbol{T_w = T_{insl},\ q_w = q_{insl}}$

(iii) Axisymmetric boundary condition, (7)

$\boldsymbol{-\lambda_f\frac{\partial T}{\partial r}\Big|_{r=0} = 0\frac{\partial u}{\partial r} = 0}$

(iv) Storage tank sidewall boundary condition, (8)

$\boldsymbol{-\lambda\frac{\partial T_{insl}}{\partial r} = h(T_{insl}-T_{amb})}$

(v) Storage tank top and bottom wall boundary condition, (9)

$\boldsymbol{-\lambda\frac{\partial T_{insl}}{\partial z} = h(T_{insl}-T_{amb})}$

Thermal losses to the ambient are determined using the following correlation for the paraboloidal domain of storage tank [16].

$$\overline{Nu} = 2+\frac{0.589Ra^{1/4}}{\left[1+(0.469/Pr)^{\frac{9}{16}}\right]^{4/9}} \tag{10}$$

The local heat transfer coefficients are evaluated at the lateral wall of the storage tank, considering the radius of curvature as the characteristic dimension at every local point. The average *Nu* is estimated based on equation (10). The initial conditions are specified as below.

$$\text{at } t=0,\ \boldsymbol{u=0},\ \boldsymbol{T=T_{ini}},\boldsymbol{T_{insl}=T_{amb}} \tag{11}$$

The ambient temperature is chosen as 27 °C. The finite element method based commercial software *COMSOL Multiphysics 5.4a* is used to solve the governing equations (1-4) using the initial and boundary conditions given by equations (5-11). Previously, this numerical model could capture the axial temperature profile of water in a stand-alone vertical cylindrical TES tank with a maximum deviation of 2.09% from the experimental data and a root mean square error of ±0.26°C [10]. For the present study, appropriate grid size and time step for the numerical model are obtained through the grid and time step independence studies. The maximum difference of 0.51% is observed for the water temperature distribution along the height of the storage tank at the end of 6 h, when grid size is decreased from fine (6503 elements) to extremely fine (17607 elements). Similarly, the temperature distribution presents a negligibly small deviation for the time steps of 1, 5 and 10 s. Therefore, the fine grid and a time step of 5 s are chosen for the present study.

SIMULATION BOX-BEHNKEN DESIGN (BBD)

Design Procedure

The objective of the designed simulations is to formulate a correlation between the multiple process parameters in order to evaluate the response. Previously, one factor at a time (OFAT) approach has been used to assess the effects of process parameters on the response. However, OFAT does not consider the effect of interaction terms on the response, which leads to inefficiency in predicting the quadratic effect of process parameters. BBD, an RSM, gives accurate results in a lesser number of simulations as compared to other approaches. Designed simulations in the BBD approach present the advantage of reduced costs and time. In the present study, a four-parameter three-level BBD is utilized to assess the effects of process parameters and their interactions on the response i.e. temperature of the water contained in the tank. The parameters considered are (i) charging temperature (*A*), (ii) ambient temperature (*B*), (iii) Height ratio (*C*), i.e., ratio of the axial height of the point of interest from the top of the tank to the total height of the tank, and (iv) storage time ratio (*D*), i.e., ratio of the specific time of interest to the total stand-alone time. Three levels are assigned to each process parameter, the levels are high, medium, and low, denoted by +1, 0 and -1,

respectively. The BBD approach suggests 27 simulation runs for the four independent process parameters. The Minitab Software Version 19.0 is used to determine the total number of simulations. The predicted response (Y) is represented as a function of independent process parameters using a second-order polynomial regression equation, as shown in equation (12) [17].

$$Y = \theta_o + \sum_{i=1}^{k} \theta_i x_i + \sum_{i=1}^{k} \theta_{ii} (x_i)^2 + \sum_{i=1}^{k-1} \sum_{j=2}^{k} \theta_{ij} x_i x_j \quad (12)$$

where, $\theta_o, \theta_i, \theta_{ii}, \theta_{ij}$ are the regression coefficients. x_i and x_j are the process parameters. The constant term, θ_o represents the intercept when all the values of process parameters (x_i) are zero. $\theta_i, \theta_{ii}, \theta_{ij}$ represent the coefficients associated with the linear, square, and interaction effects, respectively. Analysis of variance (ANOVA) is carried out to estimate the significance of the regression terms.

Development of Correlation

The coded values, which represent the individual levels of the process parameters, are used to perform the calculations and the results obtained are decoded to generate the response. The coded values for each process parameter are determined using equation (13). Based on the coded values for every numerical run, a design matrix is created consisting of linear, square and interaction terms.

$$coded\ value = \frac{e - avrg}{rng/2} \quad (13)$$

$$avrg = \frac{(Prmtr)_{max} + (Prmtr)_{min}}{2} \quad (14)$$

$$rng = (Prmtr)_{max} - (Prmtr)_{min} \quad (15)$$

where, e is the value of the process parameter. The design matrix is utilized to evaluate the coded coefficients for every term in the prediction equation.

The formulation used to obtain the design matrix and coded coefficients for the prediction model has been taken from our previous work [10]. The second column of **Table 2** presents the coded coefficients evaluated for every term (linear, square and interaction). Equations (16-18) are used to convert the coded coefficients into the uncoded coefficients.

$$Intercept_{uncoded} = Intercept_{coded} - \sum_{i=1}^{n} \left(\frac{\theta_{i,coded} e_{avg,i}}{0.5 e_{range,i}} \right) + \sum_{j=1}^{n} \sum_{i=1}^{n} \left(\frac{\theta_{ij,coded} e_{avg,i} e_{avg,j}}{0.5 e_{range,i} 0.5 e_{range,j}} \right) \quad (16)$$

$$\theta_{i,uncoded} = \frac{\theta_{i,coded}}{0.5 e_{range,i}} - \frac{2\theta_{ii,coded} e_{avg,i}}{(0.5 e_{range,i})^2} + \sum_{j=1}^{n} \left(\frac{\theta_{ij,coded} e_{avg,j}}{0.5 e_{range,i} 0.5 e_{range,j}} \right) \quad (17)$$

$$\theta_{ij,uncoded} = \frac{\theta_{ij,coded}}{0.5 e_{range,i} 0.5 e_{range,j}} \quad (18)$$

where, $\theta_{i,uncoded}$ and $\theta_{ij,uncoded}$ are the coefficients of linear and interaction terms. Multiplication of uncoded coefficients with the corresponding linear or interaction term produces the generic prediction model given in equation (12).

Table 2: Coefficients and statistical significance metrics for the regression model

Term	Coded coefficient	SE Coefficient	F-Value	P-Value
Model	-	-	7583	0
Constant	68.6	0.119	-	0
A	19.2883	0.0594	105446.3	0
B	0.2267	0.0594	14.56	0.002
C	-1.02	0.0594	294.88	0
D	-1	0.0594	283.43	0
A×A	0.0433	0.0891	0.24	0.635
B×B	0.0383	0.0891	21.36	0.047
C×C	-0.6992	0.0891	61.58	0
D×D	0.0008	0.0891	0	0.993
A×B	0.003	0.103	0	0.981
A×C	-0.36	0.103	12.24	0.004
A×D	-0.578	0.103	31.51	0
B×C	0.138	0.103	19.41	0.031
B×D	0.185	0.103	11.23	0.044
C×D	0.028	0.103	0.07	0.794

Predicted Response and Model Summary

Various metrics, such as error degrees of freedom (*Error DF*), mean square error (*MSE*), standardized effect coefficients (*SE Coeff*), total sum of squares (i.e., the sum over all the squared differences between the observations and their overall mean), error sum of squares (i.e., the sum of squares of residual values) and Coefficient of determination (R^2) are evaluated based on the formulations presented by Khurana et al. [10]. The fraction of total variation that can be explained by the fitted model is represented by the coefficient of determination. A 100% predicted R^2 denotes that the model perfectly reproduces the response of the system. On the other hand, 0% predicted R^2 denotes the overfitted model.

For every simulation, the predicted response values are obtained by substituting the values of four process parameters and their interaction terms into the prediction equation. Based on the results of designed simulation runs and the predicted responses, various plots such as versus plot, normal probability plot, versus order and Pareto charts can be created to analyze the prediction model. The normal probability plot shows the distribution of data points. Divergence from the straight line suggests a deviation from normality.

Box-Behnken Design

The numerical simulations designed by BBD are executed according to the design matrix created for three levels (-1, 0, +1) of the process parameters. The results obtained through the designed numerical simulations are analysed using the Minitab 19.0 statistical software. The uncoded coefficients are obtained from the equations (16-18). Uncoded coefficients

are substituted into the equation (12) and a prediction equation is formed. The regression equation generated is expressed in equation (19). However, analysis of variance (ANOVA) is required to evaluate the statistical significance of each term in the prediction equation, as every term may not impact the response significantly.

To determine the significance of each term, P-value and F-value are evaluated for every term in the model. The model terms with P-value less than 0.05 are considered as statistically significant. Also, the F-value of the model needs to have a substantially high value to have an impact on the response. For the present model, F-value is obtained as 7583. The high F-value along with a very low P-value of the model verifies the adequacy of the model. Based on the aforesaid criterion and ANOVA, the terms *A, B, C, D, BB, CC, AC, AD, BC,* and *BD* of the model are observed to be statistically significant. Equation (19) and (20) exhibit the full-fledged and the reduced prediction equations, respectively. The reduced model (equation (20)) considers only the significant terms. The positive and negative regression coefficients imply that the response will increase and decrease, respectively, when the specific model term increases from a lower to a higher level. The very high F-value negates the possibility of such high magnitude occurring from noise. The predicted coefficient of determination (R^2) of the model is 99.93%, which indicates that the full prediction equation has an excessive degree of fit and the variations which cannot be explained by the model are only 0.07%.

$$\begin{aligned} T = {} & 0.95 + 0.9972A - 0.071B + 1.97C + 0.31D \\ & + 0.000108A^2 + 0.00091B^2 \\ & - 2.797C^2 + 0.004D^2 \\ & + 0.000019AB - 0.036AC \\ & - 0.0594AD + 0.0423BC \\ & + 0.0585BD + 0.113CD \end{aligned} \quad (19)$$

$$\begin{aligned} T = {} & 0.95 + 0.9972A - 0.071B + 1.97C + 0.31D \\ & + 0.00091B^2 - 2.797C^2 - 0.036AC \\ & - 0.0594AD + 0.0423BC \\ & + 0.0585BD \end{aligned} \quad (20)$$

Figure 3 presents the predicted response versus the actual response for the 27 simulation runs performed. The actual response corresponds to the detailed simulation involving the governing equations, whereas the predicted response is obtained from the reduced prediction equation (equation (20)). The straight line in **Figure 3** signifies a reasonably good agreement between the prediction model and designed simulations. Therefore, the reduced prediction model enables reliable depiction of the response variable (working fluid temperature) in terms of the four key process parameters.

NUMERICAL RESULTS AND CASE STUDY

In order to have a deeper insight into the performance of the prediction model, a case study has been performed. The parameters considered in the case study are as follows: ***A*** (charging temperature) = 90 °C, ***B*** (ambient temperature) = 23 °C, ***C*** (height ratio) is varied between 0 and 1, and ***D*** (storage time ratio) is varied between 0.027 and 1.

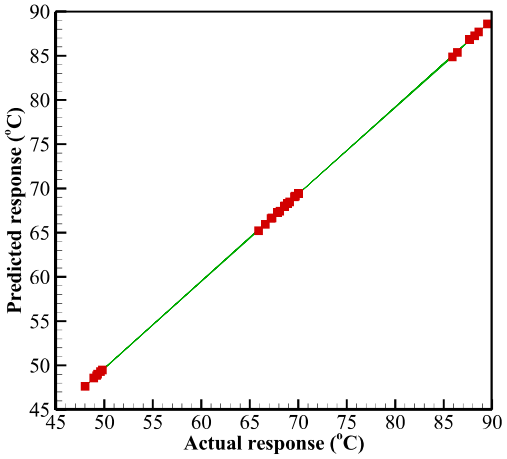

Figure 3: Plot of predicted response versus actual response

This specific case is simulated using the governing equations (Eq. 1-4) along with initial and boundary conditions (Eq. 5-11). **Figure 4** shows the volumetric temperature distribution of water inside the paraboloidal storage tank at three chosen time instants (t = 0 h, 3 h and 6 h). Water loses heat to the ambient during stand-alone operation. As the process continues, the cold water settles at the bottom, and the hot water rises to the upper section of the TES. This movement of water occurs due to the difference in densities, leading to the formation of thermal stratification in the tank. Two distinct regions form within the TES due to thermally induced buoyancy effects. One region is represented by a steep temperature gradient, which exists over a small length along the height of the lower part of the storage tank. Another region, which exists over most of the upper part of the storage tank, is represented by almost uniform temperature. The thickness of the stratified section increases with time owing to the decreased temperature gradient along the height of the storage tank. The reduced prediction equation (equation (20)) is utilized, to obtain the water temperature distribution along the height of the paraboloidal storage tank at six different time instants during the stand-alone operation. **Figure 5** exhibits the axial temperature profiles of water inside the TES tank at six different instants of stand-alone operation, obtained from the detailed simulations as well as the reduced prediction equation (20). The emergence of thermal stratification (*i.e.*, development of temperature gradient) is noticeable from the axial temperature profiles of water.

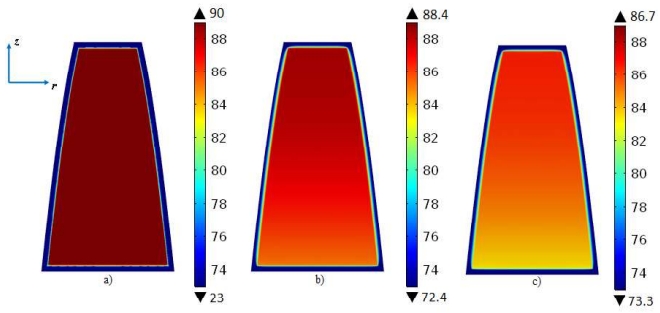

Figure 4: Water temperature (°C) distribution inside paraboloidal storage tank at (a) 0 h, (b) 3 h and c) 6 h.

The maximum root-mean-square-error (RMSE) observed between the results produced by the detailed simulation and the reduced prediction equation is ±0.13 °C. As an illustrative example, one fixed set of process parameters is used to evaluate the water temperature inside the paraboloidal storage tank at a predefined location and specific instant during the stand-alone operation. The values of the process parameters used are A=90, B= 23, C= 0.6, and D= 0.2. The temperatures obtained through the detailed numerical simulations and the reduced prediction equation (20) are 88.75 °C and 88.54 °C, respectively. Therefore, the deviation associated with the predicted response is 0.21 °C.

The axial water temperature profiles shown in **Figure 5** depict the evolution of thermal stratification inside the paraboloidal storage tank, which is reliably captured by the prediction model. The reduced prediction equation is devoid of significant computational expenses, and therefore, it can serve as an adequately accurate rapid assessment tool for evaluating the heat retention capability of the paraboloidal TES tank.

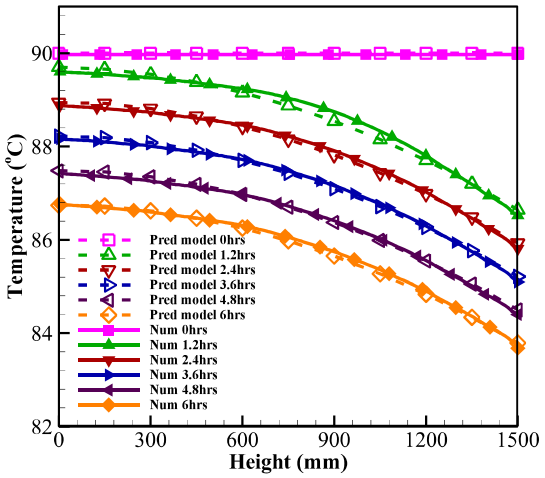

Figure 5: Axial variation of water temperature inside paraboloidal tank at different instants obtained through prediction model and detailed simulations.

CONCLUSION

In this study, a two-dimensional axisymmetric numerical model is developed for simulating a paraboloid TES tank under stand-alone mode of operation, for a total operational duration of 6 h. Formation of temperature gradient along the tank height was evident from the simulations. Volumetric temperature maps exhibited the formation of uniform temperature region and thermocline region along the tank height. This can be attributed to the continuous thermal losses to the ambient. To facilitate computational economy, a prediction model was developed based on designed simulation methodology, using a four parameter three-level Box-Behnken Design Response Surface Methodology. The developed model for the paraboloidal TES considered a wide range of values for key operating parameters, charging temperature (50-90 °C) and ambient temperature (23-26°C). A reduced prediction equation is formed by selecting only the statistically significant terms. The reduced equation enables prediction of axial temperature profiles with adequate accuracy.

REFERENCES

[1] Majumdar R, Saha SK. Reduced order heat exchanger model for low-to-medium temperature range solar thermal applications. In: Tyagi H, et al., editors. *Advances in Solar Energy Research. Energy, Environment and Sustainability, Singapore*: 2019, p 357-393.

[2] Majumdar R, Saha SK, Singh S. (2018) Evaluation of transient characteristics of medium temperature solar thermal system utilising thermal stratification. *Applied Energy* 2018; 224:69-85.

[3] Palacios A, Barrenche C, Navarro ME, Ding Y. Thermal energy storage technologies for concentrated solar power-A review from a materials perspective. *Renewable Energy* 2020; 156; 1244-1265.

[4] Kocak B, Fernandez AI, Paksoy H. Review on sensible thermal energy storage for industrial solar applications and sustainability aspects. *Solar Energy* 2020; 209; 135-169.

[5] Rosen MA, Tang R, Dincer I. Effect of stratification on energy and exergy capacities in thermal energy storage systems. *Int J of Energy Research* 2004; 28:177-193.

[6] Davis GDV. Natural convection of air in a square cavity: A benchmark numerical solution. *Int J for Numerical Methods in Fluids* 1983; 3:249-264.

[7] Mallison G, Davis GDV. Three-dimensional natural convection in a box; a numerical study. *J of Fluid Mechanics* 1977; 83:1-31.

[8] Vierendeels J, Merci B, Dick E. Numerical study of convective heat transfer with large temperature differences. *Int J of Numerical Methods in Heat and Fluid Flow* 2001; 11:329-341.

[9] Khurana H, Tiwari S, Majumdar R, Saha SK. Comparative evaluation of circular truncated-cone and paraboloid shapes for thermal energy storage tank based on thermal stratification performance. *J of Energy Storage* 2021; 34:102191.

[10] Khurana H, Majumdar R, Saha SK. Response surface methodology-based prediction model for working fluid temperature during stand-alone operation of vertical cylindrical thermal energy storage tank. *Renewable Energy* 2022; 188; 619-636.

[11] Nobel Internationals Technical Manual, Bulgaria. https://nobel.bg/ (accessed Feb 21, 2021).

[12] Rahman A, Smith AD, Fumo N. Performance modelling and parametric study of a stratified water thermal storage tank. *Applied Thermal Engineering* 2016; 100:668-679.

[13] Hang Y, Qu M, Ukkusuri S. Optimising the design of a solar cooling system using central composite design techniques. *Energy and Buildings* 2011; 43:988-994.

[14] Mutch JJ. Residential water heating: fuel conservation, economics and public policy, 1974.

[15] Kamg KU, Chung BJ. The effects of the anode size and position on the limiting currents of natural convection mass transfer experiments in a vertical pipe. *Trans of KSME B* 2010; 34:1-8.

[16] Churchill SW, Chu HSS. Correlating equations for laminar and turbulent free convection from a vertical plate. *Int J of Heat Mass Transfer* 1975;18:1323-1329.

[17] Jalalian IJ; Mohammadiun M, Moqadam HH, Mohammadiun H. Box-Behnken statistical design to optimise thermal performance of energy storage system. *Heat Mass Transfer* 2018; 54:1257-1266.